

Replacing the involute profile with an improved cycloid profile to improve the bearing capacity for the elliptical gear drives

Nguyen Hong Thai*, Phung Van Thom

*Faculty of Mechatronics, School of Mechanical, Hanoi University of Science and Technology,
No. 1, Dai Co Viet, Hai Ba Trung, Ha Noi, Viet Nam*

*Emails: thai.nguyenhong@hust.edu.vn

Received: 11 April 2023; Accepted for publication: 24 February 2024

Abstract. This paper presents an analysis and evaluation to verify the disadvantages of tooth geometry of EG drives with the involute profile. On that basis, an improved cycloid curve is applied to improve the irregularity and increase the teeth size distributed on the gear. Two prototype gear drives with the same centrodes with ellipse involute and improved cycloid profiles were manufactured and tested. The results showed that the EG drives with the improved cycloid profile allowed the design with fewer teeth than the involute profile to make the tooth size larger. Also, the experimental results showed that the practical versus theoretical gear ratio error value of the EG drives with improved cycloid profile and involute profile was 3.81 % and 6.67 %, respectively. This verified that the EG drives with the improved cycloid profile have a smoother meshing process than those with the involute profile. The research results are significant for applying and developing the improved cycloid profile in designing and manufacturing EG drives requiring high torque and precision.

Keywords: improved cycloid profile, involute profile, elliptical gear drives, geometric shapes, load capacity.

Classification numbers: 5.5.1, 5.5.3, 5.6.1.

1. INTRODUCTION

Among non-circular gears (NCGs), elliptical gears (EGs) are the most widely used due to their excellent performance. Elliptical gear pairs are used in various machines, mechanisms and equipment, flow meters, etc. In particular, they are suitable for low-speed and high-torque occasions, such as the frequency conversion vibrators of spacecraft and missile ground combat equipment and the ranging device of tank control systems [1]. Research works on the application of EGs can be mentioned as follows: Liu *et al.* proposed a pipeline robot driven by non-circular gear to modify harmonic inertia force to improve the mobility performance of the robot [2]; Prikhodko [3] investigated the dynamics of the intermittent motion conveyor mechanical system, with the mechanical transmission being an elliptical planetary gear train; Chen *et al.* [4] used an EG drive on silk reeling machine for better silk winding shape with more straightforward machine structure; Seto *et al.* [5] applied EG drives in the actuator to increase the

thermodynamic efficiency of the Stirling engine cycle; Emura and Arakawa [6] applied EGs in the steering mechanism of autonomous robots, this design helps to reduce the turning radius of the robot. In addition, Volkov *et al.* [7] and Liu *et al.* [8] used EG drives in hydraulic machine design, etc.; Zhou *et al.* designed the transplanting structure of the rice transplanter [9] and seedling transplanter [10] using the EGs gear system; Zhao *et al.* combined EGs with other NCGs applied in an automatic scallion seedling feeding mechanism for transplanting speed up to 100 plants/min with a success rate was 93.4 %. [11]; Ottaviano *et al.* [12] studied the application of EGs to replace the cam mechanism of the blood pump in cardiac surgery. Thus, elliptical gears can also be a hotspot for research on non-uniform transmission. It is predicted that elliptical gears will soon be an indispensable part of many smart products that contain mechanical parts. Nevertheless, elliptical gear drives are very speed-sensitive, and the gear ratio error and stability can be improved by decreasing speed or increasing load. This problem was pointed out by Dong *et al.* through experimental research on gear ratio characteristics of elliptical gears [13].

The above discussion shows that EGs have been used to create transmitters with the desired gear ratio function that meets practical requirements. The meshing process between pairs of conjugated profiles determines the gear ratio function of the EG drives. In previous research, the most commonly used tooth profile was the involute curve of a circle [14-16]. Also, some studies used the Novikov arc [16-19] or the involute curve of an ellipse [18]. However, the above profiles have some disadvantages, which include: (i) A large minimum number of teeth due to undercutting conditions, leading to small teeth reducing the transmission capacity, and (ii) Teeth pointed at the small radius position of the centrode. To overcome these disadvantages, Bair [20] had a positive displacement of the rack cutter during the shaping process. However, this solution creates a gap between the teeth during the meshing process and increases the axial distance of the EG drives leading to the actual gear ratio function error. When the pressure angle is small, undercutting will occur. Liu *et al.* proposed a novel variable-involute and variable-cycloid composite tooth profile based on the envelope method. The simulation results and the seedling picking experiment in the seedling pick-up mechanism verified that the tooth profile design method was feasible [21]. Through long-term and in-depth research, scholars have gradually perfected transmission theory and developed many excellent mechanisms with EGs.

Recently, to increase the load capacity of the NCG drives by increasing the dimension of the teeth, Thai *et al.* [22, 23] proposed a new curve referred to as an improved cycloid to the tooth profile of NCG. Unlike other profiles, the improved cycloid profile allows the design with a larger modulus, overcoming the phenomenon of the tooth pointed at the small radius position of the centrode and increasing the gear drive's load capacity [24]. This paper clarifies the advantages of the improved cycloid profile over the involute profile in the design of EG drives. Two EG drives with improved cycloid profile and involute profile with the same centrodes parameters were designed and manufactured to investigate and mutually verify. First, the centrodes mathematical model of the elliptical gear drives is presented. On that basis, the design of the EG drives with an involute profile and improved cycloid profile is described in Section 2. Additionally, this content also includes investigations and comparisons of the tooth geometric shapes of the involute profile versus the improved cycloid profile to clarify the irregularity of the involute profile and the advantages of the improved cycloid profile. Section 3 presents experimental results on the gear ratio function characteristics of the EG drives in the two cases. These results are then discussed and compared with the theoretical research findings for mutual verification. Section 4 presents conclusions from this study, which can serve as a basis for applying and developing the research's results in practice.

2. ELLIPTICAL GEAR DRIVES DESIGN

2.1. Centrode of the elliptical gear drives

Consider a pair of mating ellipse centrodes Σ_1 and Σ_2 , as shown in Figure 1. Wherein, Σ_1 and Σ_2 are the same centrodes Σ of the corresponding EGs in the gear drives and are determined by the polar equation [25]:

$$\rho(\phi) = \frac{2ab}{(a+b) - (a-b)\cos(2\phi)} \quad (1)$$

wherein a , b are the semi-major and semi-minor axis of Σ and the polar angle $0 \leq \phi \leq 2\pi$, respectively.

Thus, the gear ratio function of the EG drives is given by [24]:

$$i_{12}(\phi_1) = \frac{\omega_1}{\omega_2} = \frac{A((a+b) - (a-b)\cos(2\phi)) - 2ab}{2ab} \quad (2)$$

where $A = \overline{O_1O_2}$ is the distance between the rotation centers of the EG drives.

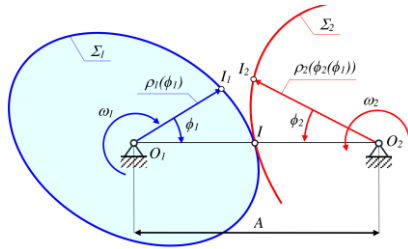


Figure 1. Illustration of mating centrodes Σ_1 and Σ_2 .

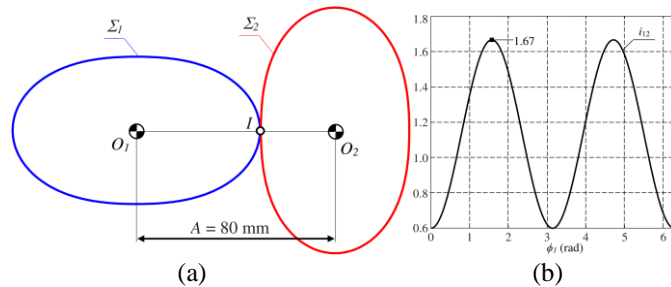


Figure 2. Design the centrode of an EG drives with (a) the centrodes, (b) the gear ratio function.

To illustrate the design method, consider EG drives with the centrode design parameters Σ : $a = 50$ mm, $b = 30$ mm. Instead of equation (2), we can determine the axis distance $A = 80$ mm. After calculating the number using the program written by the authors on Matlab, the centrode of the EG drives is described in Figure 2a, and the gear ratio function determined by the centrode of the EG drives is illustrated in Figure 2b.

2.2. Generation of elliptical gears with involute profile

The rack cutter with isosceles trapezoidal profiles shapes the involute profile for the EGs, as shown in Figure 3.

The parameters of the rack cutter are determined as follows:

1. Tooth pitch on datum line Δ of rack cutter:

$$p_c = \frac{C_\Sigma}{z} \quad (3)$$

Here $C_\Sigma = \int_0^{2\pi} \sqrt{\rho^2(\phi) + \left(\frac{d\rho(\phi)}{d\phi}\right)^2} d\phi$ is the circumference of Σ , with $\rho(\phi)$ being defined according to equation (1), and z is the number of teeth of the EGs.

2. The modulus m_c of the rack cutter:

$$m_c = \frac{p_c}{\pi} \quad (4)$$

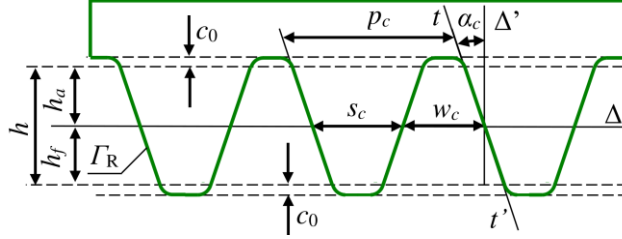


Figure 3. Parameters of rack cutter.

3. The pressure angle α_c of the rack cutter:

$$\alpha_c = \angle(tt', \Delta') \quad (5)$$

4. The whole depth of the rack cutter:

$$\begin{cases} h_a = k_a m_c \\ h_f = k_f m_c \\ h = h_a + h_f = (k_a + k_f) m_c \end{cases} \quad (6)$$

Where h_a , h_f are the addendum and dedendum of the rack cutter, respectively, with k_a and k_f being the addendum and dedendum coefficients.

5. Tooth thickness s_c and width of space w_c on the datum line Δ :

$$s_c = w_c = \frac{p_c}{2} = \frac{m_c \pi}{2} \quad (7)$$

6. Fillet radius c_o of root and tip:

$$c_o = 0.25 m_c \quad (8)$$

Nevertheless, from the literature [14, 24], to avoid the undercutting phenomenon, the modulus m_c must satisfy the inequality:

$$m_c \leq \rho_{\min} \sin^2 \alpha_c \quad (9)$$

Wherein $\rho_{\min} = \frac{ab}{2a-b}$ is the minimal radius of the centrode Σ [26].

From inequality (9), the minimal number of teeth for the EGs is obtained as follows:

$$z_{\min} = \frac{C_{\Sigma}}{\pi \rho_{\min} \sin^2 \alpha_c} \quad (10)$$

So, with the design parameters of the EG drives' centrodes as presented in Subsection 2.1. The design data of the rack cutter and EG drives are shown in Table 1 and Table 2 after satisfying the condition of undercutting avoidance.

Table 1. Design data of the rack cutter to generate the involute profile.

Parameter	Notation	Unit	Value
Module	m_c	mm	2.57
Tooth pitch	p_c	mm	8.08
Pressure angle	α_c	°	20.00
Tooth thickness	s_c	mm	4.04
Width of space	w_c	mm	4.04
Whole depth	h	mm	5.78
Tooth addendum	h_a	mm	2.57
Tooth dedendum	h_f	mm	3.21

Table 2. Design data of EG drives with the involute profile.

Parameter	Notation	Unit	Value
Module	m	mm	2.57
Number of teeth	z	--	32.00
Tooth pitch	p	mm	8.08
Tooth thickness	s	mm	4.04
Width of space	w	mm	4.04
Whole depth	h	mm	5.78
Tooth addendum	h_a	mm	2.57
Tooth dedendum	h_f	mm	3.21

Figure 4 shows the design result of EG drives with involute profile after numerical calculation on Matlab when using the design data in Tables 1 and 2 and shaped by the kinematic envelope method [14, 16]. It shows the least number of teeth that can be distributed on the gear to the tooth size max.

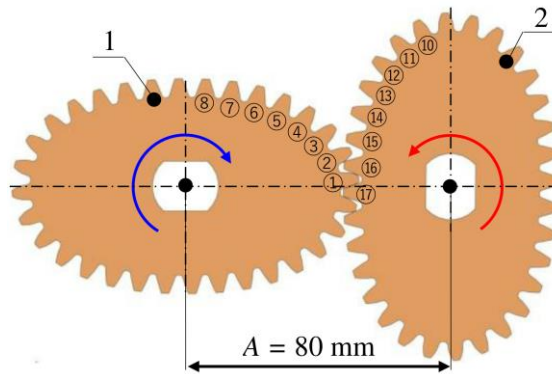


Figure 4. EG drives with an involute profile.

2.3. Investigation of tooth geometric shapes for the elliptical gears with an involute profile

Figure 4 depicts the teeth pairs involved in the meshing process when gear 1 is driven clockwise. Since the teeth are symmetrically distributed along the two semi-axes of the ellipse, the teeth on gear 1 are numbered from 1 to 8 corresponding to 17 to 10 on gear 2. Figure 5 shows tooth geometric shapes from tooth number 1 to 8 of EGs 1.

Observing Figure 5a, one obtains: (i) For the involute profile, the shape and size of teeth distributed at different positions on the EGs are not the same; (ii) The involute profile tends to increase the radius of curvature from tooth number 1 to tooth number 8. In particular, at tooth number 8, curvature profiles degenerate into a straight line the same as the rack cutter, and (iii) The most significant difference is shown on the root side, especially tooth number 1 and tooth number 8. Consequently, when transmitting the torque from the driving gear to the driven gear, as shown in Figure 5b, the weakest tooth will be the tooth at number 1.

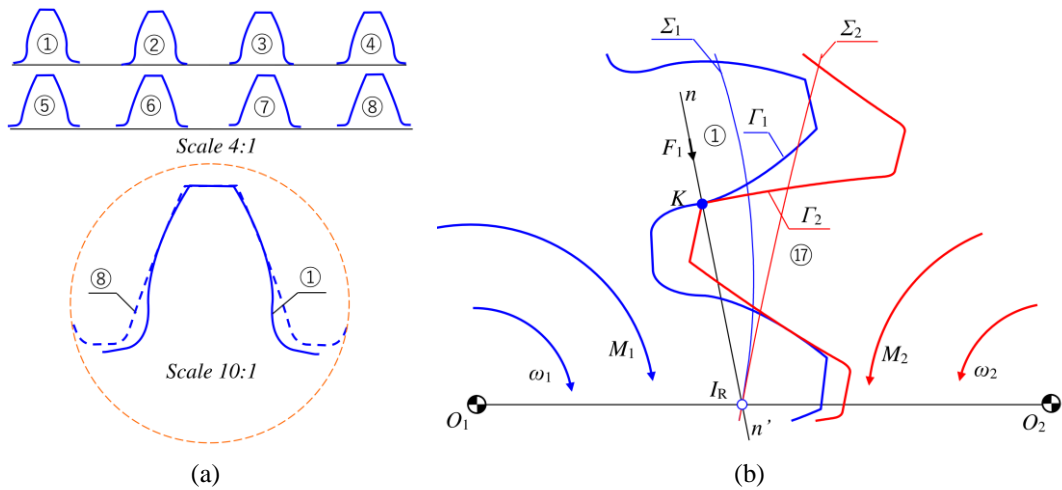


Figure 5. Difference between tooth profiles of EGs with an involute profile.

To have a more accurate assessment of the difference in the geometrical shape of the involute profile, consider two parameters related to the tooth pointed and the bearing capacity of the gear drives as the thickness of the tip and root tooth. To investigate these parameters, let s_a , s_f be the tooth tip and root thickness, respectively, as described in Figure 6. Figure 7 shows the correlation relationship between three parameters: curvature radius of the centrodes, tooth tip thickness, and tooth root thickness at positions from tooth 1 to tooth number 8 of gear 1, corresponding to teeth from 17 to 10 of gear 2.

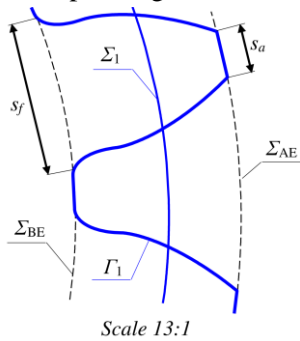


Figure 6. Illustration thickness of tooth tip and root.

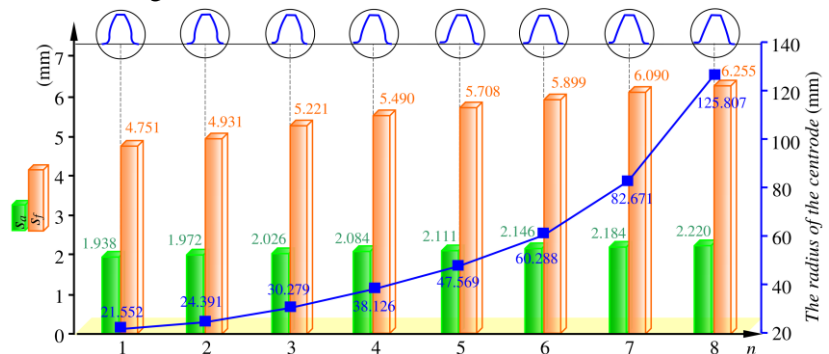


Figure 7. The tooth tip and root thickness.

From the investigation results described in the chart, Figure 7 shows that the tooth tip thickness did not change much. The thickness of tooth tip number 8 increased by 14.5 % versus tooth number 1. Meanwhile, the tooth root thickness changed significantly, specifically, the thickness of tooth root number 8 increased by 31.66 % versus tooth number 1. It means that the teeth at minimal centrodes radius have weak roots. Thus, when designing, it is necessary to pay attention to this position to increase the bearing capacity of the gear drive.

The investigation results and discussion above demonstrate that when designing EG drives with involute profiles to achieve high torque, it is only possible to enhance the material's mechanical properties but not the tooth size due to the condition of avoiding undercutting. This

study proposes to use an improved cycloid profile to address the abovementioned drawbacks of involute profiles. The next part of the paper will discuss this in more detail.

2.4. Generation of elliptical gears with an improved cycloid profile

From the definition in the literature [23], the improved cycloid curve Γ_R is generated by a fixed point K_R on the generated ellipse Σ_E as it rolls without slipping on a line Δ , as depicted in Figure 8a. The mathematical equation describing the Γ_R curve is determined by:

$$\mathbf{r}_{K_R} = \begin{bmatrix} x_{K_R} \\ y_{K_R} \end{bmatrix} = \begin{bmatrix} s_2(\phi) - a_E \sin(\psi) \\ (-1)^g s_3(\phi) - a_E \cos(\psi) \end{bmatrix} \quad (11)$$

In equation (12): $g = 0$ when Γ_R is above Δ and $g = 1$ when Γ_R is below Δ ;

$$s_2(\phi) = s_1(\phi) + r_E(\phi) \sin(\psi - \phi); \quad s_3(\phi) = r_E(\phi) \cos(\psi - \phi); \quad \psi = \phi + \mu - \frac{\pi}{2} \quad \text{with}$$

$$s_1(\phi) = \int_0^\phi \sqrt{r_E(\phi)^2 + \left(\frac{dr_E(\phi)}{d\phi} \right)^2} d\phi; \quad \mu = \tan^{-1} \left(\frac{r_E(\phi)}{dr_E/d\phi} \right)$$

is the tangent angle at the point of contact I_R of the generated ellipse Σ_E and Δ ; $r_E(\phi) = a_E \sqrt{\frac{1 - \varepsilon^2}{1 - \varepsilon^2 \cos^2 \phi}}$, wherein $\varepsilon = \frac{\sqrt{a_E^2 - b_E^2}}{a_E}$

and $a_E, b_E, \phi \in [0 \div 2\pi]$ are the major and minor axes of the generated ellipse, pole angle of the generated ellipse Σ_E , respectively [27].

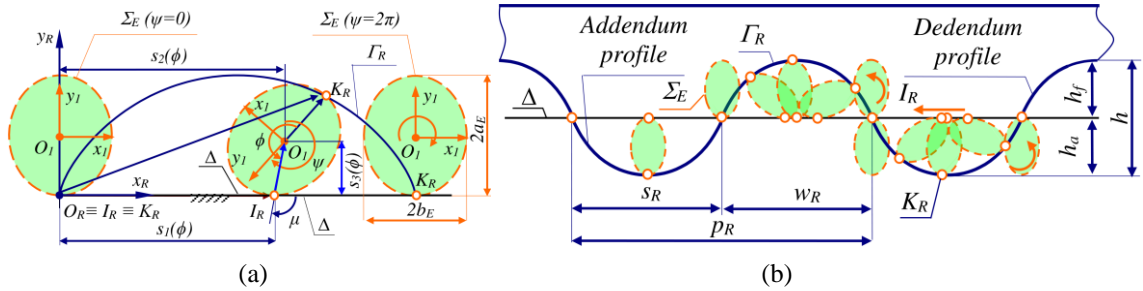


Figure 8. Novel rack cutter with (a) illustrated improved cycloid curve, (b) rack cutter with an improved cycloid profile.

Based on the improved cycloid curve, the rack cutter with the improved cycloid profile generates the tooth profile of the EGs, as depicted in Figure 8b, with the design parameters presented in Table 3.

Similar to EG drives with an involute profile presented in Subsection 2.2, the design data of the EG drives' centred hub obtained in Subsection 2.1 are also based on the design parameters in Table 3.

After distributing the number of teeth by numerical calculation and satisfying the undercutting avoidance [28] on Matlab, the design data of rack cutter and EG drives are obtained and given in Tables 4 and 5.

Table 3. Design data of improved cycloid rack cutter.

Parameter	Notation	Unit	Value
The semi-major axis of Σ_E	a_E	mm	--
The semi-minor axis of Σ_E	b_E	mm	--
Module	m_R	mm	$\frac{2}{\pi} \int_0^{2\pi} \sqrt{r_E(\phi)^2 + \left(\frac{dr_E(\phi)}{d\phi}\right)^2} d\phi$
Tooth thickness on the datum line Δ	s_R	mm	$\int_0^{2\pi} \sqrt{r_E(\phi)^2 + \left(\frac{dr_E(\phi)}{d\phi}\right)^2} d\phi$
Width of space on the datum line Δ	w_R	mm	$\int_0^{2\pi} \sqrt{r_E(\phi)^2 + \left(\frac{dr_E(\phi)}{d\phi}\right)^2} d\phi$
Tooth pitch	p_R	mm	$s_R + w_R$
Tooth addendum	h_a	mm	$\frac{ a_E b_E \cos \phi - a_E b_E }{\sqrt{(a_E \cos \phi)^2 + (b_E \sin \phi)^2}}$
Tooth dedendum	h_f	mm	$\frac{ a_E b_E \cos \phi - a_E b_E }{\sqrt{(a_E \cos \phi)^2 + (b_E \sin \phi)^2}}$
Whole depth	h	mm	$h_f + h_a$

Table 4. Design data of rack cutter with an improved cycloid profile.

Parameter	Notation	Unit	Value
The semi-major axis of Σ_E	a_E	mm	1.00
The semi-minor axis of Σ_E	b_E	mm	0.70
Module	m_R	mm	3.43
Tooth pitch	p_R	mm	10.80
Tooth thickness	s_R	mm	5.40
Width of space	w_R	mm	5.40
Whole depth	h	mm	4.00
Tooth addendum	h_a	mm	2.00
Tooth dedendum	h_f	mm	2.00

Table 5. Design data of EG drives with an improved cycloid profile.

Parameter	Notation	Unit	Value
Module	m	mm	3.43
Number of teeth	z	--	24.00
Tooth pitch	p	mm	10.80
Tooth thickness	s	mm	5.40
Width of space	w	mm	5.40
Whole depth	h	mm	4.00
Tooth addendum	h_a	mm	2.00
Tooth dedendum	h_f	mm	2.00

With the design data from Tables 4 and 5, shape the tooth profile using the kinematic envelope method in the literature [14, 23]. The resulting design of the EG drives with an improved cycloidal profile is shown in Figure 9. A comparison of the design data in Tables 2 and 5 reveals a significant reduction in the number of teeth for the EGs, from 32 to 24.

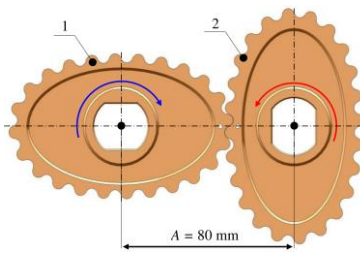


Figure 9. EG drives with an improved cycloid profile.

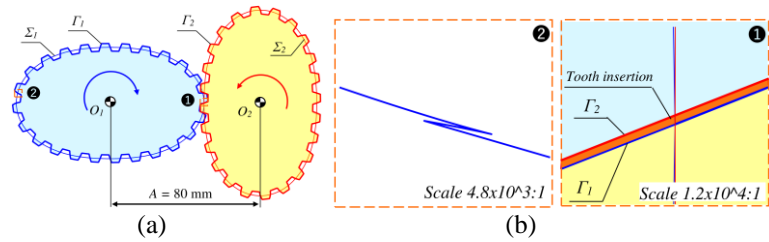


Figure 10. EG drives with an involute profile with (a) design error, (b) tooth profile interference, and tooth insertion during meshing.

Additionally, when observing Figure 9 and Figure 4, it is easy to see that the tooth size is much larger in the novel design. It shows that with the same material, the method of manufacturing EG drives with an improved cycloid profile will make the bearing capacity larger. The advantages of the improved cycloid profile over the involute profile are clarified through the design results (shown in Figure 10) of an EG drive with an involute profile using the design data in Table 5 and a pressure angle $\alpha_C = 20^\circ$.

The design results in Figure 10 show that the EG drives with an involute profile cause tooth profile interference (see Figure 10b) and get tooth insertion during the meshing process (see Figure 10c). The analysis and discussion results presented above once again confirm the advantages of an improved cycloid profile over the involute profile in enhancing the bearing capacity of EG drives.

3. TESTING THE MESHING PROCESS

In reality, the tooth profile directly influences the quality of the gear ratio function when the gear drive is in operation. Hence, the results of experimental measurements of the meshing process are presented below for two prototypes manufactured by design, as shown in Figure 4 and Figure 9.

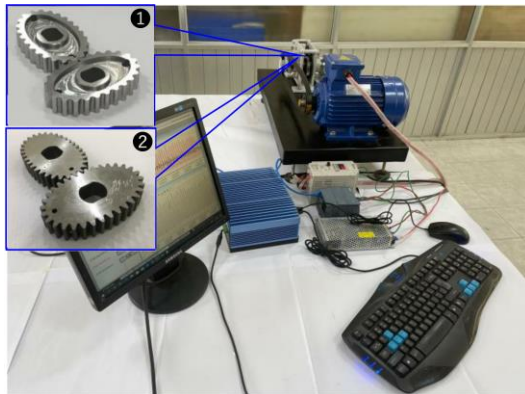


Figure 11. Experimental system.

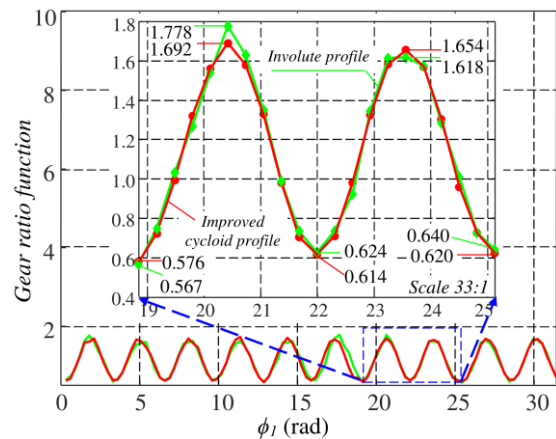


Figure 12. Experimental gear ratio.

The measuring system consists of hardware devices, as shown in Figure 11, where ① is an EG drive with an improved cycloid profile, and ② is an EG drive with an involute profile. The rotational speed of the gear shafts is determined independently by the encoders with a resolution of 400 pulses (E6B2-CWZ6C). Measurement data from the encoders is collected through the

counter of a PLC (S7-1200, CPU 1214C). The data of the PLC is transmitted to the industrial computer (BOXER-6640-A1-1010) for processing through a software written by the authors on the TIA Portal V15.1 platform. A 3-phase motor (1.5Kw) drives the shaft of the active gear through a belt transmission, and the motor speed is controlled by a Delta inverter (VFD-015M23A). The EG drive is lubricated by shell Gadus S2 V220-2 multi-purpose grease.

Set the sampling period T to 0.1 sec and the motor speed to 45 rpm, corresponding to the frequency value f set for the inverter at 1.5 Hz. Figure 12 shows a graph of the gear ratio measured at 105 points during the meshing of two EG drives in 5 revolutions of the drive gear. From Figure 12, we can see that the geometrical shape, the value, and the empirical gear ratio law are similar to the theoretical gear ratio function in Figure 2b.

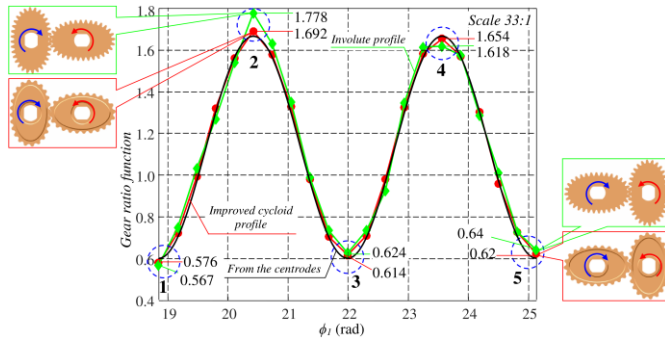


Figure 13. Comparison of theoretical and experimental gear ratios for two EG drives.

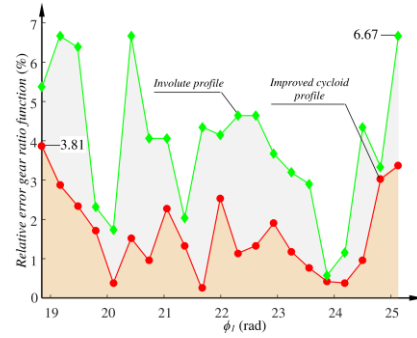


Figure 14. The error value of experimental versus theoretical gear ratios of two EG drives.

Figure 13 compares the results obtained during the 4th cycle when the system operated steadily. At times ①, ②, ③, ④, and ⑤, the relative errors between the experimental and theoretical results were 3.81 %, 1.52 %, 2.33 %, 0.76 %, and 3.37 %, respectively, for the improved cycloid profile. Meanwhile, for the involute profile, the errors were 5.43 %, 6.67 %, 4.00 %, 2.94 %, and 6.67 %. The chart in Figure 14 below describes the experimental versus theoretical gear ratio error value during the meshing process of the two gear drives.

The above experimental results indicate that the EG drives with the improved cycloid profile have a smoother meshing process than those with the involute profile.

4. CONCLUSIONS

From the simulation and experimental results verification, discussion, and evaluation above. The main conclusions obtained from this work are as follows: (1) The improved cycloid profile can design with a large modulus than the involute profile resulting in a larger tooth dimension which increases the load capacity of the elliptical gear drives; (2) The experimental results have verified that the gear ratio function error of the EG drives with an involute profile is larger than that with the improved cycloid profile. In this particular case, the max error value of the EG drives gear ratio function between experimental and theoretical are 3.81 % for the improved cycloid profile and 6.67 % for the involute profile. It means that the improved cycloid profile's meshing quality has improved.

The research results provide a theoretical basis and certain significance for applying and developing the improved cycloid profile in designing and manufacturing EG drives requiring high torque and precision. However, some aspects still need further investigation, such as the stress distribution, strain and pressure in the meshing process. Also, the vibration and noise of

the teeth that will appear in the meshing process at high speeds is also an issue worthy of further study. Thus, it will be considered part of our future research goals.

Acknowledgments. This work was supported by Hanoi University of Science and Technology, under grant number T2018-PC-021.

CRedit authorship contribution statement. Nguyen Hong Thai made the initiative idea, theoretical modeling, and implementation plan, designed the experiments, and writing of the paper. Phung Van Thom programmed and simulated, prepared tables and figures, performed experiments. Both authors discussed the results, reviewed and approved the final version of the manuscript.

Declaration of competing interest. The authors declare that they have no known competing financial interests or personal relationships that could have appeared to influence the work reported in this paper.

REFERENCES

1. Dong C., Liu Y., and Wei Y. - Dynamic contact characteristics analysis of elliptical cylinder gear under different load conditions, *Journal of Huazhong University of Science and Technology* **47** (2019) 103-107. <https://doi.org/10.13245/j.hust.190820>.
2. Liu D., Lu J., Cao Y., and Jin X. - Dynamic characteristics of two-mass impact pipeline robot driven by non-circular gears, *Advances in Mechanical Engineering* **14** (5) 2022. <https://doi.org/10.1177/16878132221095913>.
3. Prikhodko A. - Dynamic analysis of intermittent-motion conveyor actuator, *Actuators* **10** (8) 2021. <https://doi.org/10.3390/act10080174>.
4. Chen J. N., Yan J. J., Sun L., and Zhou M. - Analysis of a novel traverse mechanism driven by non-circular gears with Fourier pitch-line applied on silk reeling machine, In *Applied Mechanics and Materials* **536** (2014) 1295-1300. <https://doi.org/10.4028/www.scientific.net/AMM.536-537.1295>.
5. Zare S., Tavakolpour-Saleh A. R., Aghahosseini A., and Mirshekari, R. - Thermoacoustic Stirling engines: A review, *International Journal of Green Energy* **20** (1) (2023) 89-111. <https://doi.org/10.1080/15435075.2021.2021414>.
6. Emura T., and Arakawa A. - A new steering mechanism using noncircular gears, *JSME international journal. Ser. 3, Vibration, control engineering, engineering for industry* **35** (4) (1992) 604-610. <https://doi.org/10.1299/jsmec1988.35.604>.
7. Volkov G. Y., Fadyushin D. V. - Improvement of the method of geometric design of gear segments of a planetary rotary hydraulic machine, In *Journal of Physics: Conference Series* **1889** (4) (2021) 042052. <https://doi.org/10.1088/1742-6596/1889/4/042052>.
8. Liu D., Ba Y., and Ren T. - Flow fluctuation abatement of high-order elliptical gear pump by external noncircular gear drive, *Mechanism and Machine Theory* **134** (2019) 338-348. <https://doi.org/10.1016/j.mechmachtheory.2019.01.011>.
9. Zhou M., Yang Y., Wei M., and Yin D. - Method for generating non-circular gear with addendum modification and its application in transplanting mechanism, *International Journal of Agricultural and Biological Engineering* **13** (6) (2020) 68-75. <https://doi.org/10.25165/j.ijabe.20201306.5659>.
10. Zhou M., Hua Z., Wang J., Wang L., Zhao Y., and Yin D. - New type of transverse moving box mechanism for pot seedling transplanting machine, *Int J. Agric & Biol Eng.* **11** (2) (2018) 70-75. <https://doi.org/10.25165/j.ijabe.20181102.2867>.

11. Zhao X., Ye J., Chu M., Dai L., and Chen J. - Automatic Scallion Seedling Feeding Mechanism with an Asymmetrical High-order Transmission Gear Train, *Chin. J. Mech. Eng.* **33** (10) 2020. <https://doi.org/10.1186/s10033-020-0432-9>.
12. Ottaviano E., Lanni C., Tavolieri C., Mundo D., Danieli G., Fanghella P., and Ceccarelli M. - An Experimental Comparative Study on Non-Circular Gears and Cam Transmissions for a Blood Pumping System, In *International Design Engineering Technical Conferences and Computers and Information in Engineering Conference* **42568** (2006) 371-380. <https://doi.org/10.1115/DETC2006-99166>.
13. Dong C., Pei W., Liu Y., Wei Y., Li D., Guo R., and Ren Z. - Experimental Research on Transmission Characteristics of Elliptic Gear Transmission Systems, *Strojniški vestnik- Journal of Mechanical Engineering* **68** (11) (2022) 702-712. <https://doi.org/10.5545/sv-jme.2022.332>.
14. Litvin F. L., Gonzalez-Perez I., Fuentes A., and Hayasaka K. - Tandem design of mechanisms for function generation and output speed variation, *Computer methods in applied mechanics and engineering* **198** (5-8) (2009) 860-876. <https://doi.org/10.1016/j.cma.2008.10.010>.
15. Colbourne J. R - *The Geometry of Involute Gears*, Springer, New York, 1987.
16. Litvin F. L., Gonzalez-Perez I., Fuentes A., Hayasaka K. - Design and investigation of gear drives with non-circular gears applied for speed variation and generation of functions, *Computer methods in applied mechanics and engineering* **197** (45-48) (2008) 3783-3802. <https://doi.org/10.1016/j.cma.2008.03.001>.
17. Korotkin Viktor I., Nikolay P. Onishkov, and Yuri D. Kharitonov - *Novikov gearing: Achievements and development - Novikov Gearing: Achievements and Development*, Nova Science Publishers Inc, New York, 2011.
18. Viktor I. Korotkin , Nikolay P. Onishkov, Yury D. Kharitonov - *Novikov Gearing Achievements and Developments*, Nova Science Pub Inc, 2011.
19. Bair B. W., Sung M. H., Wang J. S., and Chen C. F. - Tooth profile generation and analysis of oval gears with circular-arc teeth, *Mechanism and machine theory* **44** (6) (2009) 1306-1317. <https://doi.org/10.1016/j.mechmachtheory.2008.07.003>.
20. Bair B. W. - Computer aided design of non-standard elliptical gear drives, *Proceedings of the Institution of Mechanical Engineers, Part C: Journal of Mechanical Engineering Science* **216** (4) (2001) 473-482. <https://doi.org/10.1243/0954406021525250>.
21. Liu J. G., Tong Z. P., Yu G. H., Zhao X., and Zhou H. L. - Design and application of non-circular gear with cusp pitch curve, *Machines*, **10** (11) (2022) 985. <https://doi.org/10.3390/machines10110985>.
22. N. H. Thai, P. V. Thom, N. T. Trung - Influence of centrodes coefficient on the characteristic of gear ratio function of the compound non-circular gear train with improved cycloid tooth profile, In *IFTToMM Asian conference on Mechanism and Machine Science*, Springer, 2021, pp. 204-214. https://doi.org/10.1007/978-3-030-91892-7_19.
23. N. H. Thai, N. T. Trung - A novel curve for the generation of the non-circular gear tooth profile, *International Journal of Engineering* **35** (5) (2022) 1024-1036. <https://doi.org/10.5829/IJE.2022.35.05B.18>.

24. N. H. Thai, P. V. Thom - Research on the Characteristics of Tooth Shape and Size of the Oval Gear Drive with an Involute Profile, In Regional Conference in Mechanical Manufacturing Engineering, Springer, 2022, pp. 167-184. https://doi.org/10.1007/978-981-19-1968-8_14.
25. Vanegas-Useche L. V., Abdel-Wahab, M. M., and Parker, G. A. - A new noncircular gear pair to reduce shaft accelerations: A comparison with sinusoidal and elliptical gears, *Dyna* **83** (198) (2016) 219-227. <https://doi.org/10.15446/dyna.v83n198.49170>.
26. Thai N. H., Long N. D. - A new design of the Lobe pump is based on the meshing principle of elliptical gear pairs, *Science & Technology Development Journal-Engineering and Technology* **4** (2) (2021) 861-871. <https://doi.org/10.32508/stdjet.v4i2.769>.
27. Litvin F. L., Alfonso Fuentes-Azna, Ignacio Gonzalez-Perez, Kenichi Hayasaka. - *Noncircular Gears Design and Generation*, Cambridge University Press, New York, 2009.
28. Faydor L. Litvin, Alfonso Fuentes - *Gear Geometry and Applied Theory*, Cambridge University Press, New York, 2004.